

## Altered Metabolomic Profiles May Be Associated with Sevoflurane-Induced Neurotoxicity in Neonatal Rats

Bin Liu · Yuechao Gu · Hongyan Xiao ·  
Xi Lei · Weimin Liang · Jun Zhang

Received: 19 November 2014/Revised: 23 January 2015/Accepted: 28 January 2015/Published online: 7 February 2015  
© Springer Science+Business Media New York 2015

**Abstract** Experimental studies demonstrate that inhaled anesthetics can cause neurodegeneration and neurobehavioral dysfunctions. Evidence suggests changes in cerebral metabolism following inhaled anesthetics treatment can perturb cerebral homeostasis, which may be associated with their induced neurotoxicity. Seven-day-old rat pups were divided into two groups: control group (Group C) and sevoflurane group (Group S, 3 % sevoflurane exposure for 6 h). Gas chromatography–mass spectrometry (GC–MS) was used for analyzed differential metabolites of cerebral cortex in both groups. Also western blot, flow cytometry, enzymatic methods and electron microscopy were performed in various biochemical and anatomical assays. Sevoflurane exposure significantly elevated caspase-3 activation and ROS levels, decreased mitochondrial cardiolipin

contents, and changed cellular ultrastructure in the cerebral cortex. Correspondingly, these results corroborated the GC–MS findings which showed altered metabolic pathways of glucose, amino acids, and lipids, as well as intracellular antioxidants and osmolyte systems in neonatal brain following prolonged exposure to high sevoflurane concentration. Our data indicate that sevoflurane anesthesia causes significant oxidative stress, neuroapoptosis, and cellular ultrastructure damage which is associated with altered brain metabolome in the neonatal rat. Our study also confirmed that GC–MS is a strategic and complementary platform for the metabolomic characterization of sevoflurane-induced neurotoxicity in the developing brain.

**Keywords** Metabolome · Sevoflurane · Developing brain · Gas chromatography · Neurotoxicity

Bin Liu and Yuechao Gu have contributed equally to this work.

B. Liu · H. Xiao · X. Lei · W. Liang · J. Zhang (✉)  
Department of Anesthesiology, Huashan Hospital, Fudan University, No. 12 Wulumuqi Middle Road, Jin'an District, Shanghai 200040, People's Republic of China  
e-mail: snapzhang@aliyun.com

B. Liu  
e-mail: lbzaixuzhou@126.com

H. Xiao  
e-mail: hongyanxiao@yahoo.cn

X. Lei  
e-mail: anesthesia2006xi@163.com

W. Liang  
e-mail: chiefliang@yahoo.com.cn

Y. Gu  
Department of Anesthesiology, Shanghai Cancer Hospital, Fudan University, Shanghai 200032, People's Republic of China  
e-mail: yuechaogu@126.com

### Introduction

Mounting experimental studies demonstrate that commonly used general anesthetics, especially inhaled anesthetics, could trigger widespread apoptotic neurodegeneration in the developing brain, and cause long-term neurobehavioral abnormalities in rodents [1–5] and nonhuman primates [6, 7]. However, the cellular mechanisms of general anesthetics-induced neurotoxicity are not fully clarified.

General anesthesia can greatly influence cerebral metabolism in many ways [8–10]: cerebral blood flow-metabolism uncoupling, reduction in regional cerebral metabolic oxygen rate, glucose utilization, and oxidative adenosine triphosphate (ATP) production rate in animals and humans in a dose-dependent manner. Given their influence on brain metabolism, anesthetics may perturb cerebral homeostasis, and thus may be associated with

inhaled anesthetic-induced neurotoxicity. Therefore, it is vitally important to understand the effects of inhaled anesthetics on cerebral metabolism in the developing brain.

Although anesthesia disrupts many metabolic processes, like those mentioned above, the effects of other metabolic pathways in the brain remain unknown. Metabolomics recently has been introduced to study the small-molecule metabolite profiles of biological organisms [11]. This method can be applied to elucidate changes of metabolites in the brain of animals exposed to neurotoxins and provide information to identify early and differential markers for disease [12].

By using proton magnetic resonance spectroscopy ( $^1\text{H}$ MRS), Makaryus et al. [13] analyzed cerebral metabolites in rats and children [14] during general anesthesia and found that inhaled and intravenous anesthetics produce distinct metabolomic profiles in some brain regions such as parietal cortex and hippocampus. Here we hypothesize the alternation in cerebral metabolism underlie potential changes in anatomical/biochemical characteristics after inhaled anesthetics treatment, and these neurochemical sequelae may be involved in inhaled anesthetic-induced neurotoxicity [15]. To test our hypothesis, we applied gas chromatography–mass spectrometry (GC–MS) analysis to assay brain metabolites in neonatal rats, intended to identify the early metabolic phenotypes following prolonged exposure to high sevoflurane concentration. Sevoflurane, a commonly used inhaled anesthetic in clinical paediatric anesthesia, has been reported to have neurotoxic property on developing brain. Further, we examined apoptotic markers, oxidative status, and ultrastructural properties in a neonatal rat model to gain a better insight into the pathogenesis of sevoflurane-induced neurotoxicity.

## Materials and Methods

### Chemicals and Reagents for Metabolomic Analysis

Methanol (pesticide residue grade), bis-(trimethylsilyl)-trifluoroacetamide (BSTFA) plus 1 % trimethylchlorosilane (TMCS) (REGIS Technologies Inc. Morton Grove, IL, USA), and amino acid standard solution were purchased from Sigma-Aldrich (St. Louis, MO, USA). L-2-chlorophenylalanine (internal standard) was obtained from Shanghai Hengbai Biotech Co. Ltd. (Shanghai, China). All other chemicals and reagents were purchased from Anpel Company (Shanghai, China). Distilled water was prepared using the Milli-Q Reagent-Water System (Millipore, MA, USA).

### Animals and Anesthesia

Sprague–Dawley (SD) rats used in the present study were obtained from the Animal Care Center of Fudan

University. The study protocol was reviewed and approved by the Institutional Animal Care and Use Committee, Fudan University. According to the flow chart of the experimental protocol (Fig. 1), the rat pups (body weight:  $12.1 \pm 0.1$  g) at postnatal day 7 (P7) were divided into two groups: control (Group C) and sevoflurane-treated (Group S).

P7 rats in group S were placed in a sealed chamber ventilated with 3 % sevoflurane in 100 % oxygen for 6 h and sevoflurane concentration was continuously measured through a gas sample line by using a monitor (Datex Ohmeda S/5, Helsinki, Finland) whereas those in group C were placed in a similar chamber for 6 h under identical experimental conditions without sevoflurane exposure. The temperature in the sealed chamber was maintained at 33–35 °C with a heating pad. The total survival percentage of P7 rats in group S after 6-h anesthesia was 90 %. After treatment, the rat pups were returned to their dams for lactation. The rats in the same litter were used for each experiment and they were sacrificed by rapid decapitation at 12 h after sevoflurane exposure. The frontal cortex was harvested and stored at –80 °C until use. The preparations of the brain samples and the number of animals used were described in their methods, respectively.

### Blood Gas Analysis

P7 rats ( $n = 4$  each group) were used to assess the effect of sevoflurane treatment on arterial blood gases. Arterial blood sampling from the left cardiac ventricle was performed immediately after the end of sevoflurane anesthesia according to the previous described method [16]. We measured partial pressures of carbon dioxide ( $\text{PaCO}_2$ ) and oxygen ( $\text{PaO}_2$ ), pH, and blood lactate and glucose levels with a Radiometer ABL 800 blood gas analyzer (Radiometer, Copenhagen, Denmark).

### GC–MS Analysis

Prior to metabolic profiling, frontal cortex ( $n = 6$ /group) were homogenized with 50  $\mu\text{L}$  L-2-chlorophenylalanine in a 2-mL centrifuge tube. Then, 0.4 mL methanol-chloroform (3:1, V:V) as extraction liquid was added to each homogenate. After 2 min of vortex-mixing, the samples were centrifuged at 12,000 rpm for 10 min at 4 °C and 400  $\mu\text{L}$  of supernatant from each sample was transferred into a new 2-mL glass tube. The supernatants of cortical samples were concentrated to complete dryness at a temperature of 50 °C for approximately 30 min using the TurboVap nitrogen evaporator (Caliper Life Science, Hopkinton, MA). Afterward, 100  $\mu\text{L}$  of anhydrous toluene (stored with sodium sulfate) was added to each of the dried tissues. Following 1 min of vortex-mixing, the samples

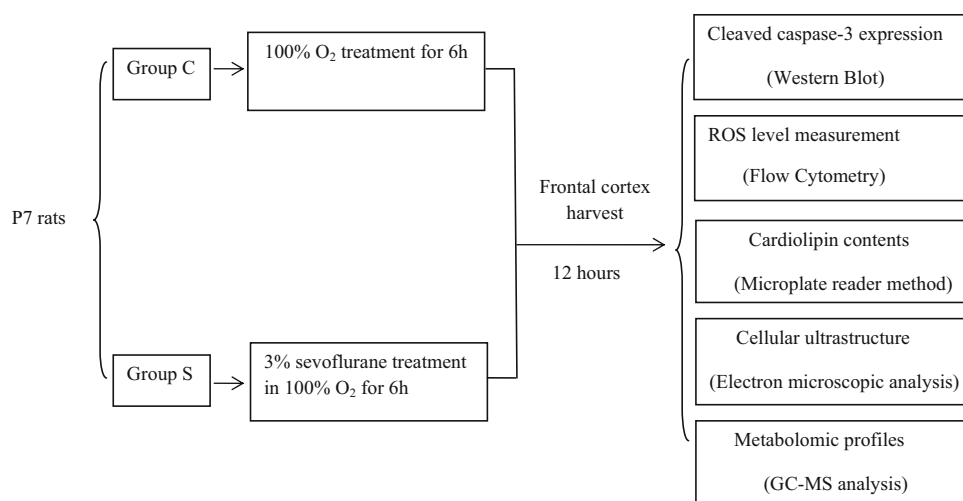


**Fig. 1** Flow chart of experimental protocol

were evaporated to dryness using the evaporator to ensure the complete elimination of any traces of water which might interfere with the subsequent GC–MS analysis. Then, 80  $\mu$ L MOX reagent was added to the dried samples, vortex-mixed for 2 min, and incubated at 37  $^{\circ}$ C for at least 2 h as a methoximation step. Derivatization reaction aimed to increase the volatility of polar metabolites was then initiated by adding 100  $\mu$ L of BSTFA (with 1 % TMCS) to each sample, vortex-mixed for 2 min, and incubated at 70  $^{\circ}$ C for 60 min. Following the incubation, each sample was vortex-mixed for 2 min and carefully transferred to the autosampler vials for subsequent GC–MS analysis [17].

GC–MS analysis was performed on an Agilent 7890A gas chromatography system coupled with an Agilent 5975C mass spectrometer (Agilent, USA). The system utilized a DB-5MS capillary column coated with 5 % diphenyl cross-linked with 95 % dimethylpolysiloxane (30  $\mu$ m  $\times$  250- $\mu$ m inner diameter, 0.25- $\mu$ m film thickness; J&W Scientific, Folsom, CA, USA). A 1- $\mu$ L aliquot of the analyte was injected in splitless mode. Helium was used as the carrier gas, the front inlet purge flow was 3 mL/min, and the gas flow rate through the column was 1 mL/min. The initial temperature was kept at 80  $^{\circ}$ C for 2 min, then raised to 240  $^{\circ}$ C at a rate of 5  $^{\circ}$ C/min, and finally to 290  $^{\circ}$ C at a rate of 10  $^{\circ}$ C/min for 11 min. The injection, transfer line, and ion source temperatures were 280, 270, and 220  $^{\circ}$ C, respectively. The energy was  $-70$  eV in electron impact mode. The mass spectrometry data were acquired in full-scan mode with the  $m/z$  range of 20–600 at a rate of 100 spectra per second after a solvent delay of 492 s. Chroma TOF4.3X software of LECO Corporation were used to acquire mass spectrometric data [18]. Mass spectra of all detected compounds were compared with spectra in the National Institute of Standards and Technology (NIST,

<http://www.nist.gov/index.html>) and Fiehn databases. The peaks with similarity index of more than 70 % were selected and named the putative metabolite identities.

#### Multivariate Data Analysis

The resulting GC–MS data were first processed by normalizing peak area of each analyte based on total integral area calculation performed using an in-house script (Microsoft Office Excel). All processed data were then mean-centered and unit-variance scaled before they were subjected to principal component analysis (PCA) (version 11.5, SIMCA-P software, Umetrics, Umea, Sweden) to identify clustering trend, as well as detect and exclude outliers. Quality control (QC) samples for cortical tissues were prepared by randomly pooling 5  $\mu$ L from each of the five samples belonging to the test groups. QC samples were analyzed at constant intervals to ensure that the data acquisition for GC/MS metabolic profiling was reproducible for all samples. Variable importance in the projection (VIP) cutoff value was defined as 1.00.

#### Western Blot Analysis

The frontal cortical tissues were homogenized in RIPA buffer (Millipore, Temecula, CA, USA) containing complete protease inhibitor cocktail and 2 mM phenylmethylsulfonyl fluoride. The lysates were collected and centrifuged at 12,000 rpm for 30 min at 4  $^{\circ}$ C. After the protein samples were quantified using a BCA Protein Assay Kit (Pierce Biotechnology, Rockford, IL, USA), the cleaved caspase-3 expression was detected by western blot analysis according to our previous method [4]. Data were expressed as mean  $\pm$  SD. The changes were presented as a

percentage of those of the control group. One-hundred-percent of caspase-3 activation refers to control level for the purpose of comparison to that in Group S.

#### Measurement of ROS Levels

The frontal cortex was cleaned in PBS and dissociated in trypsin solution, and stopped using DMEM solution. A single-cell suspension was obtained by using a 70- $\mu\text{m}$  mesh. The chemiluminescent probe with flow cytometry technique was used for detection of intracellular ROS level according to a previously described method [19]. Briefly, 2',7'-dichlorofluorescein diacetate (DCFH-DA) probe was added to the cell suspensions at a final concentration of 10  $\mu\text{mol/L}$  and incubated at 37 °C, protected from light for 1 h, followed by flow cytometry (FACSCanto, BD Biosciences, San Jose, CA, USA) measurement. The formation of the oxidized fluorescent derivative 2',7'-dichlorofluorescein (DCF) was monitored with excitation light at 488 nm and emission light at 525 nm, and normalized by protein concentration. By quantifying fluorescence intensity of DCF, the ROS levels in both groups were calculated.

#### Mitochondrial Cardiolipin Assay

Extraction of mitochondria was performed using the mitochondria isolation kit (Shanghai Genmed Scientifics Inc., China). Briefly, the frontal cortex was lysed in precooled centrifuge tubes and disrupted by 80 passes in the homogenizer with a tight fitting Dounce homogenizer. The homogenate was then centrifuged for 10 min at 1,500g at 4 °C. The mitochondria-rich supernatant was then collected and centrifuged for 10 min at 10,000g at 4 °C. The mitochondrial pellets were then washed with 2 mL of preservation medium (25 mmol/L potassium phosphate; 5 mmol/L  $\text{MgCl}_2$ , pH 7.2) and centrifuged for 5 min at 10,000g at 4 °C. Purified mitochondrial samples were freeze-thawed three times and suspended to 5.5 mg/mL in PBS before use. The mitochondrial cardiolipin contents were quantified by the microplate reader method using the high affinity 10-*N*-nonyl acridine orange (NAO) for cardiolipin of freshly isolated mitochondria [20]. Briefly, reagents (90  $\mu\text{L}$ ) from cardiolipin assay kits (Shanghai GenMed Scientifics Inc., Shanghai, China) was added into mitochondrial sample (10  $\mu\text{L}$ ) on the microplate. The microplate was gently shaken and incubated in a dark room for 20 min at room temperature. Then fluorescence intensity was measured with excitation light at 580 nm and emission light at 630 nm. The cardiolipin contents were expressed as relative fluorescence unit (RFU) and normalized by protein concentration.

#### Electron Microscopy

The rat brain was perfused with normal saline solution followed by phosphate-buffered 2.5 % glutaraldehyde and 4 % paraformaldehyde 12 h after sevoflurane treatment, then the frontal cortex was sliced into sections of approximately 1  $\text{mm}^2$ , and kept in the same glutaraldehyde solution for 12 h at room temperature. Samples were postfixed in 1 % osmium tetroxide for 2 h, dehydrated in a series of alcohol solutions at 4 °C, immersed in propylene oxide, and embedded in Araldite 502 resin at 60 °C. Ultrathin (0.5  $\mu\text{m}$ ) sections were placed on grids and stained with uranyl acetate and lead citrate before examination with a transmission electron microscope (Philips CM-120, Eindhoven, The Netherlands). The organelles of neuronal cells were observed and imaged at 10,000 $\times$  magnification.

#### Statistical Analysis

We performed one-way ANOVA to determine differences in caspase-3 activation and cardiolipin contents, and independent Student's *t* test to compare the difference in arterial blood gas analysis and ROS levels. Independent *t* tests with Welch's correction were then used for statistical comparison of discriminant metabolite levels between Group C and Group S, which determined for sevoflurane-induced alteration of metabolic profiling in neonatal rat model. The significance level was set at  $p < 0.05$ .

## Results

#### Blood Gas Analysis

The Table 1 showed the results of arterial blood gas analysis and biochemical parameters from neonate rats in both groups immediately after sevoflurane treatment. Data from arterial blood analysis revealed that 6 h sevoflurane anesthesia did not induce significant disturbances in

**Table 1** Arterial blood gas and biochemical parameters in control and anesthetized neonatal rats ( $n = 4/\text{group}$ )

	Group C	Group S
PH	7.41 $\pm$ 0.12	7.19 $\pm$ 0.08*
PaO <sub>2</sub> (mmHg)	398.7 $\pm$ 53.4	175.0 $\pm$ 10.8
PaCO <sub>2</sub> (mmHg)	38.8 $\pm$ 5.2	81.9 $\pm$ 8.4*
Blood glucose (mmol/L)	5.58 $\pm$ 1.56	6.33 $\pm$ 0.75
Blood lactate (mmol/L)	0.35 $\pm$ 0.04	0.42 $\pm$ 0.10

Data presented as Mean  $\pm$  SD. Statistic analysis with independent student *t* test, compared with Group C

\*  $p < 0.05$

oxygenation, blood glucose and lactate. However, compared with Group C, exposure to 3 % sevoflurane for 6 h caused significant hypercapnia and acidosis in neonatal rats.

### Sevoflurane Alters the Metabolomic Profiles

#### Data Processing and Pattern Recognition

The representative GC–MS chromatogram of a cortical sample of a sevoflurane-treated P7 rat depicting the peaks of discriminate metabolites is shown in Fig. 2 with the major metabolites noted.

PCA of brain samples indicated that the cerebral cortex in sevoflurane-treated and control neonatal rats formed two distinct clusters on the scores plot. In order to obtain a higher level of group separation and get a better understanding of the variables responsible for classification, a supervised partial least squares discriminant analysis (PLS-DA) was employed, and spectral profiles were readily distinguished between Group S and Group C (Fig. 3a). PLS-DA is commonly used for classification purposes and biomarker selection in metabolomics studies. If a statistically significant discrimination between two groups can be found, then the model parameters can be interpreted for their discriminating power and metabolic biomarkers can be found. The classification parameters from the software were  $R^2X = 0.710$ ,  $R^2Y = 0.975$ , and  $Q^2 = 0.834$ , which were stable and good to fitness and prediction. A sevenfold cross-validation was used to estimate the robustness and the predictive ability of our model. To further validate our model, we performed 200 permutations, and the  $R^2$  and the  $Q^2$  intercept values were (0.0, 0.679) and (0.0, 0.091) for the cerebral cortex (Fig. 3b), which indicates that the PLS-DA models in this study have good or excellent fitness and predictive abilities. These

results demonstrate that GC–MS-based metabolomic analysis is well-suited to detect sevoflurane-induced brain metabolic alterations in neonatal rat.

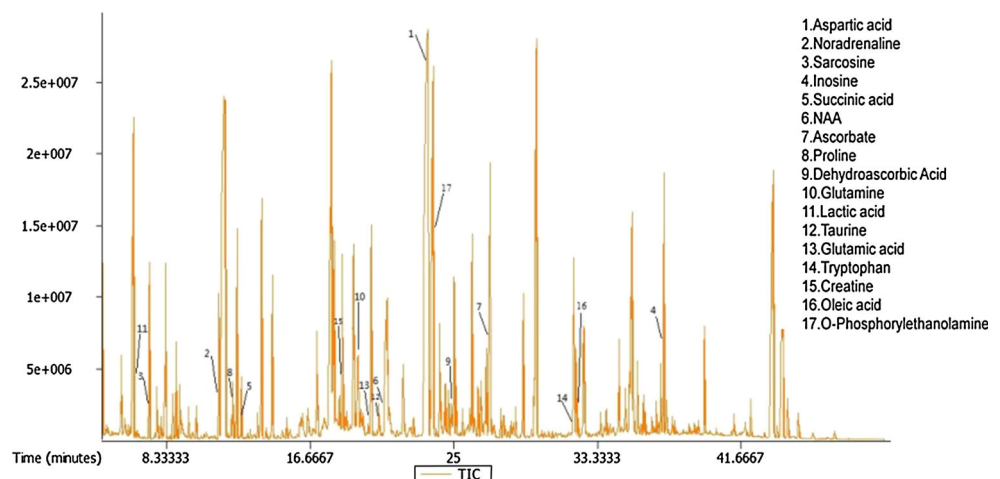
#### Metabolic Profiling

GC–MS analysis provided the metabolic profiles of neonatal brains in both groups. A set of discriminant brain metabolites that was responsible for distinguishing sevoflurane-treated rats from control ones in the PLS-DA model was identified. The 26 metabolites were picked out by PLS-DA ( $VIP > 1$ ) and  $t$  test ( $p$  value  $< 0.05$ ), and 16 metabolites were selected for their correlation with molecular and structural aspects of sevoflurane-induced neurotoxicity, involving in energetic metabolism, neuronal apoptosis, oxidative stress, and cell swelling. They were used to make the heatmap (Fig. 4) and summarized in Table 2 with their classifications. These metabolites were related to metabolic pathways of glucose, amino acids and lipids (phospholipids), as well as intracellular antioxidants and osmolyte systems. Next, we determined whether the changes we found in metabolism underlie potential changes in anatomical/biochemical features (neuroapoptosis, oxidative stress, and cellular ultrastructure damage) after sevoflurane treatment.

#### Sevoflurane Increases Neuronal Apoptosis

Caspase-3 activation is an indicator of cellular apoptosis [21]. Compared with Group C, 3 % sevoflurane treatment for 6 h significantly increased cleaved caspase-3 levels in cerebral cortex of Group S (Fig. 5). Our results suggest prolonged exposure to high sevoflurane concentration dramatically increased the incidence of apoptosis in the cerebral cortex of neonatal rat.

**Fig. 2** The typical spectrum from frontal cortex extract in a neonatal rat. NAA *N*-acetyl-L-aspartic acid





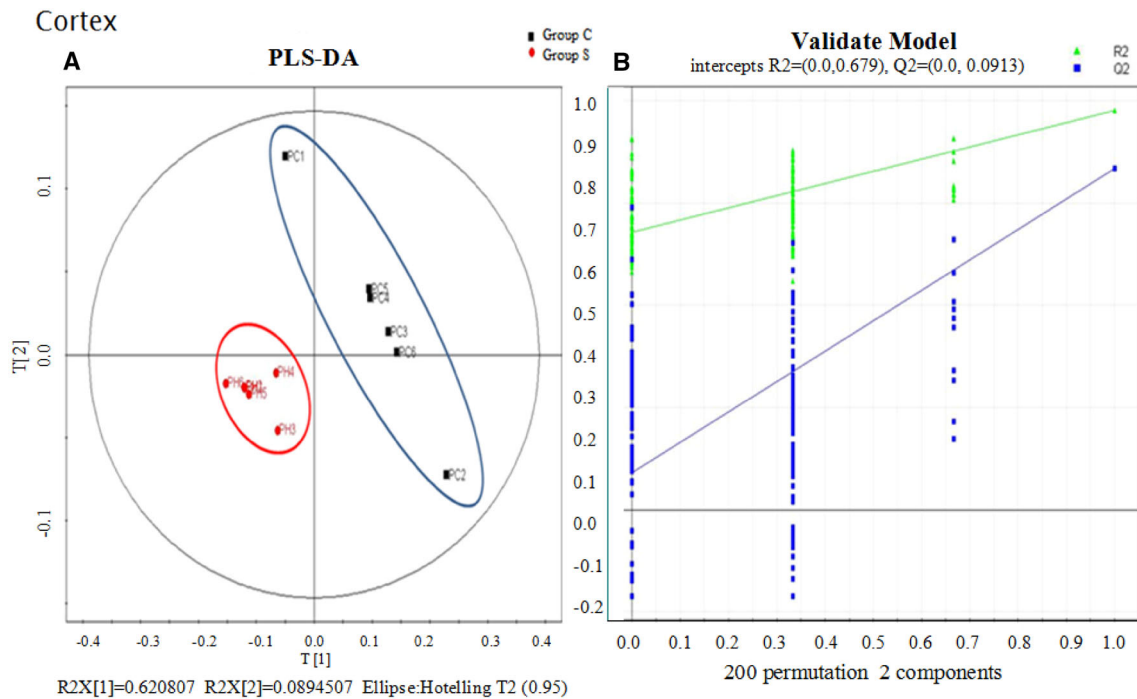


**Fig. 3** Data processing and pattern recognition of metabolomic analysis between the two groups. **a** Partial least squares projection to latent structures and discriminant analysis (PLS-DA) scores plot of cerebral cortex in neonatal rats. The statistical data analysis resulted

in a cluster formation at the two treatments. The replicates ( $n = 6/$  each group) represent untreated controls (Group C) and high concentration sevoflurane exposure (Group S). **b** Validation of the model with a permutation test

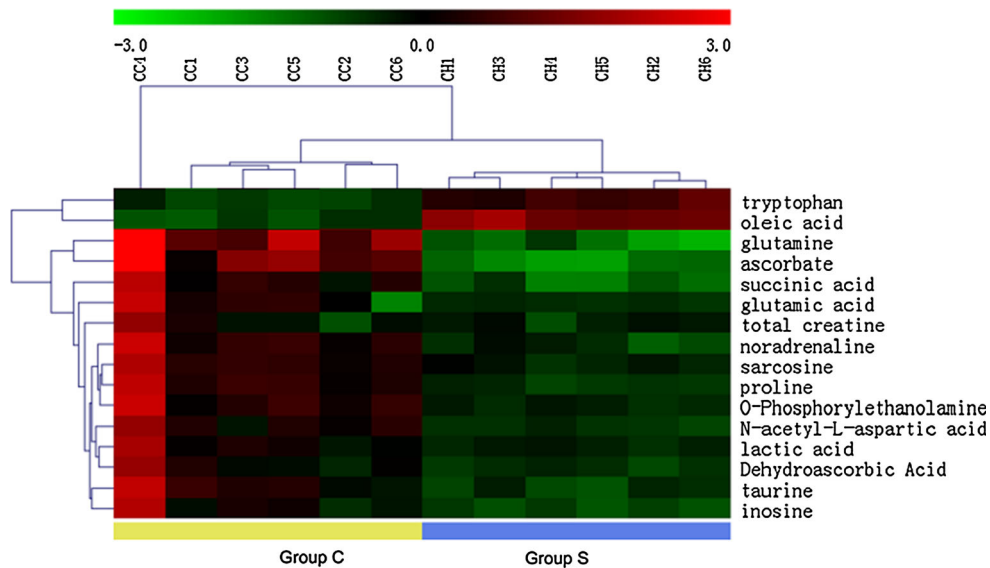


**Fig. 4** Heatmap of differential metabolites between Group S and Group C. Heatmap showing differential metabolites from cerebral cortex in Group S paired with metabolites in Group C. Each row represents one metabolite, and each column represents one tissue sample. The relative metabolite level is depicted according to the color scale. Red indicates upregulation; green indicates

downregulation. 3.0, 0, and  $-3.0$  are fold changes in the corresponding spectrum. CC1-CC6 represent tissues 1–6 from Group C, whereas CH1-CH6 represent tissues 1–6 from Group S. The different metabolites clearly self-segregated into Group C and Group S clusters. Independent  $t$  test with Welch’s correction (significance at  $p < 0.05$ )

**Sevoflurane Increases Oxidative Stress**

To test oxidative stress status, we measured total ROS levels after sevoflurane treatment. We found that the total

ROS level in cerebral cortex significantly increased after 3 % sevoflurane treatment for 6 h, compared with that in Group C (Fig. 6). To further evaluate the effect of increased generation of ROS after sevoflurane exposure, we

**Table 2** marker metabolites found in GC/MS analysis of brain samples of sevoflurane exposure and control neonatal rats

Metabolites	RT (min)	Chemical class	Identified by	% Change of Group S from control	<i>p</i> value	Similarity	VIP
Lactic acid	6.35012	Organic acid	Fiehn databases	−23.0	0.016203	904	1.44735
Sarcosine	7.28777	Amino acid	Fiehn databases	−19.4	0.033741	985	3.2138
Noradrenaline	11.3467	neurotransmitter	Fiehn databases	−31.5	0.041111	937	4.29261
Proline	12.1510	Amino acid	Fiehn databases	−33.1	0.011095	935	2.18524
Succinic acid	12.6381	Dicarboxylic acid	Fiehn databases	−53.1	0.006009	904	3.14927
Total creatine	18.5306	Organic acid	Fiehn databases	−20.8	0.037678	800	1.0311
Glutamine	19.3965	Amino acid	Fiehn databases	−58.8	0.008508	828	1.53816
Glutamic acid	20.1758	Amino acid	Fiehn databases	−30.0	0.002963	839	1.26475
Taurine	20.6277	Organic acid	Fiehn databases	−35.6	0.008136	745	1.30407
<i>N</i> -acetyl-L-aspartic acid	21.0327	Amino acid	Fiehn databases	−33.2	0.002821	879	2.8725
<i>O</i> -Phosphorylethanolamine	23.7303	Sphingolipid	NIST	−24.2	0.004955	852	3.22187
Dehydroascorbic acid	24.9923	Hydroxy acid	Fiehn databases	−33.0	0.00668	889	1.94691
Ascorbate	27.0483	Hydroxy acid	Fiehn databases	−64.0	0.003216	724	2.22106
Tryptophan	31.8846	Amino acid	Fiehn databases	60.0	0.017015	919	1.16551
Oleic acid	32.0865	Organic acid	NIST	170.0	0.001782	792	1.00714
Inosine	37.1657	Nucleoside	Fiehn databases	−43.3	0.002179	861	3.1662

RT retention time, VIP variable importance in the projection

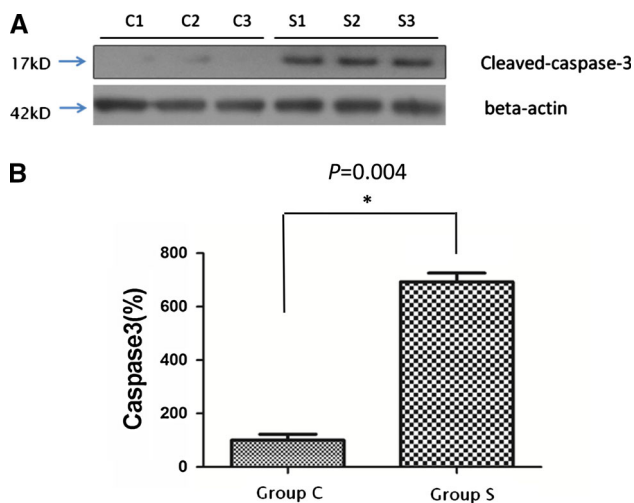


**Fig. 5** Neonatal exposure to sevoflurane increases neuroapoptosis. **a** The cortical cleaved caspase-3 expression in neonatal brain was examined with western blot. **b** Quantification of cleaved caspase-3 (one-way ANOVA,  $F = 0.607$ ,  $p = 0.004$ ),  $*p < 0.05$  Group C ( $100.0 \pm 11.4\%$ ,  $n = 3$ ) versus Group S ( $687.2 \pm 25.1\%$ ,  $n = 3$ )

measured isolated mitochondrial cardiolipin contents of the cerebral cortex. Cardiolipin, a unique mitochondrial phospholipid involved in mitochondrial energy metabolism, is a critical target of mitochondrially-generated ROS and regulates signaling events related to apoptosis [22]. We discovered that cardiolipin contents in Group S were greatly reduced when compared to Group C (Fig. 7). Combined

these two findings suggest that oxidative stress is increased in the neonatal brain exposed to sevoflurane.

#### Ultrastructural Features in Cerebral Cortex After Sevoflurane Exposure

In Group S, electron micrographs of the cerebral cortex showed ultrastructural features of typical cellular swelling. We observed hallmarks of cellular swelling in Group S, including local swelling, is recognized by a pale and watery cytoplasm under electron microscopic analysis, and swollen organelles, including dilated rough endoplasmic reticulum (RER) fragments (Fig. 8a), and increased vacuolated and swollen mitochondria (Fig. 8b); these changes were observed in both cell bodies and the neuropil of bilateral frontal cortex in Group S, but not in Group C. Interestingly, sevoflurane treatment also significantly decreased the number of synaptic vesicles at axon terminals (Fig. 8c).

#### Discussion

The present study aimed at investigating metabolic changes occurring in the cortical region of neonatal rat brain after prolonged exposure to high concentration sevoflurane using GC–MS analysis. P7 rat, a common animal model used for studying inhaled anesthetic-induced neurotoxicity, was applied in this study. As we know, frontal cortex helps mediate encoding in episodic memory and retrieval from

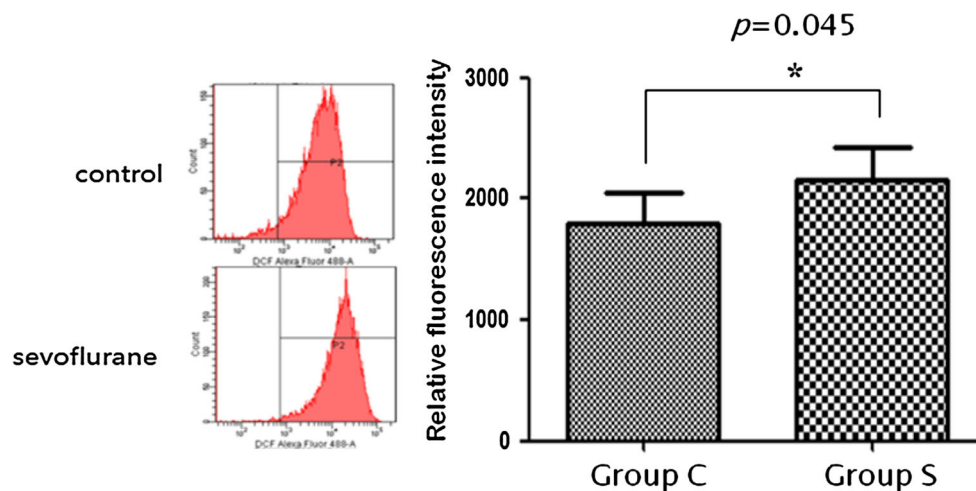


**Fig. 6** Neonatal exposure to sevoflurane increases ROS levels. The cortical ROS levels in neonatal brain were examined with flow cytometry. *Left* is formation of oxidized fluorescent derivative 2',7'-dichlorofluorescein (DCF) monitored with flow cytometry. *Right* is comparison of relative fluorescence intensity of DCF between Group

C ( $1795.5 \pm 114.1$ ,  $n = 5$ ) and Group S ( $2153.7 \pm 103.8$ ,  $n = 7$ ). The relative fluorescence intensity represents relative ROS levels in cerebral cortex. \* $p < 0.05$  Group C versus Group S (independent student *t* test, *t* value = 2.296,  $p = 0.045$ )

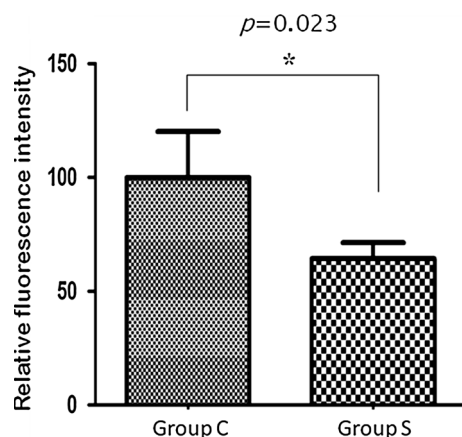


**Fig. 7** Neonatal exposure to sevoflurane reduces mitochondrial cardiolipin contents. The mitochondrial cardiolipin contents in neonatal brain were determined enzymatically in Group C ( $100 \pm 20.2\%$ ,  $n = 4$ ) and Group S ( $64.4 \pm 6.9\%$ ,  $n = 4$ ). The relative fluorescence unit represents relative mitochondrial cardiolipin contents in cerebral cortex. \* $p < 0.05$  Group C versus Group S (One-way ANOVA,  $F = 8.45$ ,  $p = 0.023$ )

episodic memory (working memory), and is involved in many higher cognitive functions [23]. The neuronal apoptosis and structure damage at early birth period in this brain region could influence its later development and subsequently neurocognitive function in adulthood. Therefore, frontal cortex was selected as a target brain region. Previous studies have showed that changes in metabolic profiling during general anesthesia in human and rodent brains [13, 14]. Because long-term neurobehaviour impairment has been reported following inhaled anesthetic

exposure [1, 3, 4], the effects of anesthesia on cerebral metabolism is assumed also persist for a relative long time. However, the characterization of cerebral metabolomics during recovery from anesthesia remain unclear, the brain samples harvested 12 h after sevoflurane anesthesia were used for this purpose.

We found that alteration in metabolite levels in the frontal cortex of neonatal rats in response to sevoflurane exposure. These changes may underlie sevoflurane-induced oxidative stress, cellular ultrastructure damage, and neuroapoptosis that we observed under the same anesthetic exposure in the developing brain. Previous studies have implicated that regional abnormalities of brain metabolites were associated with some neurological disorders [24]. Here, we found GC-MS-based metabolomics analysis, to the best of our knowledge, is first time used to characterize effects of anesthetic agents on the developing rodent brain. The PLS-DA model robustly differentiated the metabolic profiles in the sevoflurane group from the control group. The method was subsequently applied to elucidate characteristic metabolites, which has the potential to map perturbations of neurochemical changes in the developing brain [25]. This can prove to be a useful technique for investigating brain metabolic changes on exposure to general anesthetics. Remarkably, we found differential metabolites identified with altered metabolism of glucose, amino acids, and lipids, as well as intracellular antioxidants and osmolyte systems. The changes in metabolomics provided potential evidences of sevoflurane-induced developmental neurotoxicity including ultrastructural damage, oxidative stress and neuroapoptosis.



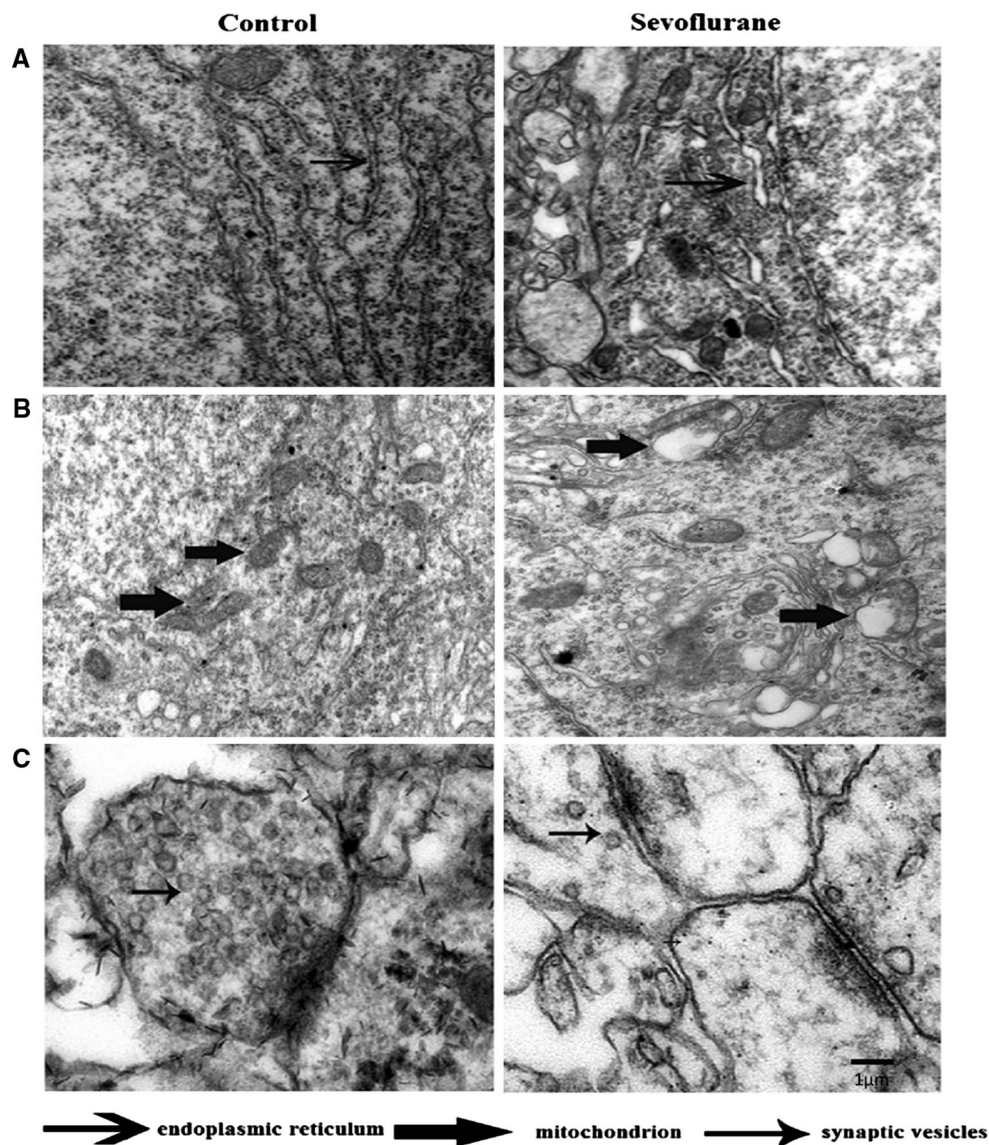


**Fig. 8** Ultrastructural changes in cerebral cortex following 3 % sevoflurane treatment for 6 h. Compared with control, neonatal exposure to sevoflurane results in dilated RER fragments (a),

increased vacuolated and swollen mitochondria (b) and reduction in number of synaptic vesicles (c) in neurons (magnification  $\times 10,000$ )

### Cellular Swelling

A number of factors have been implicated in cellular swelling [26]. One important factor is mitochondrial dysfunction, in particular the opening of the mitochondrial permeability transition (mPT) pore [27], characterized by an increase in permeability of the inner mitochondrial membrane to small solutes (ions and molecules, reducing equivalents) [28]. The mPT may lead to osmotic swelling of the mitochondrial matrix [29], mitochondrial dysfunction, defective oxidative phosphorylation, impaired ATP synthesis, and the generation of free radicals [30] which can subsequently lead to cell swelling. Myo-inosine and taurine are thought to regulate intracellular volume and

osmolarity [31]. Our GS-MS results showed a decrease in concentration of both these intracellular osmolytes in Group S, indicating alterations in intracellular osmolarity. Osmotic changes, which are associated with an influx of extracellular water into the intracellular compartment leading to cell swelling and irreversible cell damage [32], are thus likely caused by prolonged exposure to high sevoflurane concentration. This was found by electron micrographs of cerebral cortex that revealed swelling of the RER and mitochondria, similar to results in the frontal cortex following  $N_2O$  (70 %) combined with isoflurane (1 %) treatment for 8 h in nonhuman primates [6]. The cellular edema could be deleterious to neuronal and glial functioning.

## Oxidative Stress

ROS generation is part of the normal cellular metabolism in brain. However, the imbalance between production of ROS and the protective effect of the antioxidant system responsible for their neutralization and removal result in oxidative stress. Our metabolomic analysis revealed reduced intracellular levels of nonenzymatic antioxidants, ascorbate and dehydroascorbic acid, in sevoflurane-exposed neonatal brain, which may result from their consumption against ROS overload. Previous studies found that inhaled anesthetics induced neuroapoptosis through overproduction of ROS [33, 34]. In this study, we found prolonged exposure to high sevoflurane concentration significantly increased ROS levels and reduced mitochondrial cardiolipin contents, one of markers of oxidative stress in the cerebral cortex of neonatal rat. Cardiolipin is a unique tetra-acyl phospholipid that is found almost exclusively in the inner mitochondrial membrane where it is required for optimal mitochondrial function. It is particularly susceptible to ROS attack due to its high content of unsaturated fatty acids, resulting in increased membrane lipid peroxidation and reduced efficiency in mitochondrial oxidative phosphorylation [35]. There are considerable evidences suggest that an imbalance between oxidants and antioxidants play a role in the pathogenesis of several neurological disorders, such as Alzheimer's disease, Parkinson's disease, multiple sclerosis et al. [36, 37]. Several studies demonstrated that supplement of antioxidants, for example, melatonin [38], and omega-3 fatty acids [4] or ROS scavenger EUK-134 [39] could protect neuronal cells from anesthetics-induced neurotoxicity. From the perspective of metabolomics, impaired intracellular antioxidant system may play a role in reduced ability to remove free radicals and subsequent occurrence of oxidative stress.

## Neuroapoptosis

In our metabolomic analysis, we found that sevoflurane significantly reduced *O*-phosphorylethanolamine (75.8 % of control), an ethanolamine derivative that is used to construct sphingomyelins, and led to a compensatory increase in oleic acid (2.7 fold of control). Also, decline of *N*-acetyl-L-aspartic acid (NAA) levels, a marker of neuronal viability, in Group S implies neuronal loss following sevoflurane treatment. All these results seem to suggest that prolonged exposure to high sevoflurane concentration could increase neuroapoptosis or inhibit neuronal growth [40]. Correspondingly, activation of caspase-3 in frontal cortex in Group S suggests increase in neuronal apoptosis after exposure to 3 % sevoflurane for 6 h, which is consistent with results in previous findings. The number

reduction of neurons and inhibition of cell proliferation in the neonatal period could lead to behavioral deficits in adulthood.

## Metabolism Inhibition

As one of the most metabolically active organs, the brain depends on a continuous supply of energy to stabilize ionic homeostasis, energy consuming biochemical reactions, and physiological processes [41]. Hence, even a slight impairment in energy metabolism can have dramatic effects on the brain. Due to difference in affected tissues, glucose levels in ABG analysis seem not significantly change, however, the metabolomic results showed intermediates including lactate (77.0 % of control) and succinic acid (46.9 % of control) levels in the glucose metabolic pathway significantly decreased 12 h after sevoflurane anesthesia in Group S compared with Group C. As a result, the total creatine pool, including creatine and high-energy phosphocreatine, also reduced to 79.2 % of control. Its depletion could increase cellular vulnerability to insufficiency of ATP synthesis, causing cellular dysfunction [42]. In addition to as an indicator of neuronal damage, NAA has also been reported as a biomarker for mitochondrial status [43], hence a decrease in NAA might also be linked to mitochondrial dysfunction and altered neuronal energy metabolism [44]. Correspondingly, electron microscopy analysis suggested possible damaged mitochondria after sevoflurane treatment, exhibiting increased vacuolation and swelling. As the mitochondrion is often described as the "cellular power plant", its dysgenesis is one of the first signs of neuronal dysfunction [45], and has widespread consequences on many critical cellular events including essential roles in ROS level upregulation and apoptosis.

As well, altered amino acid metabolism in the neonatal brain may also play a role in sevoflurane-induced neurotoxicity. Prolonged exposure to high sevoflurane concentration significantly reduced levels of glutamine (41.2 % of control), glutamic acid (70.0 %), aspartic acid (75.7 %), and proline (66.9 %). Given their intermediate roles in the Krebs cycle [46], this decrease paralleled the reduction of lactate and succinic acid levels. Since these amino acids are also involved in the synthesis of proteins, peptides, and fatty acids, reduction of their levels suggests neuronal growth inhibition in developing brain. The changes in glutamine–glutamate, noradrenaline, and tryptophan levels suggest glutamatergic, noradrenergic, and serotonergic neurotransmission may be affected in Group S. Glutamate, playing a decisive role in the consolidation of memory, is primarily of neuronal origin [47]; therefore, decrease in glutamate levels, which might be due to leakage of glutamate from damaged neurons (may account for the reduced number of synaptic vesicles we observed at the electron

microscopy level), changed glutamate receptor functioning, altered synaptic activity, abnormal glutamine–glutamate cycling or dysfunctional glutamate transport, might result in altered learning and memory functions of the brain. These findings suggest altered synaptic transmission that may contribute to abnormal synaptic plasticity and cognitive impairments observed in rats treated with inhaled anesthetics during the neonatal period. Another non-essential amino acid sarcosine, a glycine transporter I inhibitor, also decreased compared with Group C, which may be involved in recognition and memory impairments [48]. Therefore our results also suggest pathways involved in neuronal energy metabolism can be investigated as therapeutic targets for inhaled anesthetic-induced acute widespread neurodegeneration.

### Study Limitations and Conclusion

There are some limitations to our study. First, blood gas abnormalities including hypercarbia and oxygenation depression were found during sevoflurane exposure. Previous report indicated inhaled anesthetic-induced brain cell death may be partly caused by these effects [49], which may also produce profound metabolic effects on the neonatal brain. We cannot exclude this possibility, as we did not include a carbon dioxide inhalation group. Second, a time series of metabolomic analysis following anesthesia could better help to understand a time-course for sevoflurane-induced activation of the different metabolic pathways in developing brain. And finally, we performed the metabolomic analysis on the frontal cortex only. Metabolic changes in other susceptible brain regions, for example, other cerebral cortex or hippocampus, may also be involved in sevoflurane-induced neurotoxicity. Also, as anesthetic exposure differentially induces apoptotic cell death in different brain regions [50], uncorroborated assumption that sevoflurane affects metabolism equally in all brain cells renders the association of the observed metabolomic changes and caspase-3 expression may be speculative in this study.

In conclusion, GC–MS-based metabolomic analysis can be used for studying anesthetic effects on the developing brain. The inhalational anesthetic sevoflurane treatment produced a significant metabolic signature in neonatal brains, altering metabolic pathways of glucose, lipids, and amino acids, intracellular antioxidant and osmolyte systems. These metabolic interactions in the developing brain may be of particular importance during its growth spurt period since they are essential in neuronal survival, neurogenesis, and even neurotransmission in the brain. Importantly, GC–MS can be used to screen for metabolites altered by anesthetics, which can complement anatomical and functional approaches. Although we did not use these

differential metabolites to predict biochemical/cellular damages following sevoflurane treatment, metabolomic analysis which incorporates other analysis, such as proteomics, can better interpret our findings in this study.

**Acknowledgments** This work was supported by Natural Science Foundation of China (to Jun Zhang, No. 81171020). Thanks for assistance of Biotree Biotechnology Co. Ltd (Shanghai, China) on GC–MS analysis.

**Conflict of interest** Bin Liu, Yuechao Gu, Hongyan Xiao, Xi Lei, Weimin Liang and Jun Zhang reported no conflicts of interest.

### References

- Jevtovic-Todorovic V, Hartman RE, Izumi Y, Benschoff ND, Dikranian K, Zorumski CF, Olney JW, Wozniak DF (2003) Early exposure to common anesthetic agents causes widespread neurodegeneration in the developing rat brain and persistent learning deficits. *J Neurosci* 23:876–882
- Zhou ZW, Shu Y, Li M, Guo X, Pac-Soo C, Maze M, Ma D (2011) The glutaminergic, GABAergic, dopaminergic but not cholinergic neurons are susceptible to anaesthesia-induced cell death in the rat developing brain. *Neuroscience* 174:64–70
- Shen X, Liu Y, Xu S, Zhao Q, Guo X, Shen R, Wang F (2013) Early life exposure to sevoflurane impairs adulthood spatial memory in the rat. *Neurotoxicology* 39:45–56
- Lei X, Zhang W, Liu T, Xiao H, Liang W, Xia W, Zhang J (2013) Perinatal supplementation with omega-3 polyunsaturated fatty acids improves sevoflurane-induced neurodegeneration and memory impairment in neonatal rats. *PLoS One* 8:e70645
- Zheng H, Dong Y, Xu Z, Crosby G, Culley DJ, Zhang Y, Xie Z (2013) Sevoflurane anesthesia in pregnant mice induces neurotoxicity in fetal and offspring mice. *Anesthesiology* 118:516–526
- Zou X, Liu F, Zhang X, Patterson TA, Callicott R, Liu S, Hanig JP, Paule MG, Slikker W Jr, Wang C (2011) Inhalation anesthetic-induced neuronal damage in the developing rhesus monkey. *Neurotoxicol Teratol* 33:592–597
- Brambrink AM, Evers AS, Avidan MS, Farber NB, Smith DJ, Zhang X, Dissen GA, Creeley CE, Olney JW (2010) Isoflurane-induced neuroapoptosis in the neonatal rhesus macaque brain. *Anesthesiology* 112:834–841
- Lenz C, Rebel A, van Ackern K, Kuschinsky W, Waschke KF (1998) Local cerebral blood flow, local cerebral glucose utilization, and flow-metabolism coupling during sevoflurane versus isoflurane anesthesia in rats. *Anesthesiology* 89:1480–1488
- Kaisti KK, Långsjö JW, Aalto S, Oikonen V, Sipilä H, Teräs M, Hinkka S, Metsähonkala L, Scheinin H (2003) Effects of sevoflurane, propofol, and adjunct nitrous oxide on regional cerebral blood flow, oxygen consumption, and blood volume in humans. *Anesthesiology* 99:603–613
- Du F, Zhu X, Zhang Y, Friedman M, Zhang N, Ugurbil K, Chen W (2008) Tightly coupled brain activity and cerebral ATP metabolic rate. *Proc Natl Acad Sci USA* 105:6409–6414
- Nicholson JK, Lindon JC (2008) Systems biology: metabolomics. *Nature* 455:1054–1056
- Chang KL, New LS, Mal M, Goh CW, Aw CC, Browne ER, Chan EC (2011) Metabolic profiling of 3-nitropropionic acid early-stage Huntington's disease rat model using gas chromatography time-of-flight mass spectrometry. *J Proteome Res* 10:2079–2087
- Makaryus R, Lee H, Yu M, Zhang S, Smith SD, Rebecchi M, Glass PS, Benveniste H (2011) The metabolomic profile during

- iso-flurane anesthesia differs from propofol anesthesia in the live rodent brain. *J Cereb Blood Flow Metab* 31:1432–1442
14. Jacob Z, Li H, Makaryus R, Zhang S, Reinsel R, Lee H, Feng T, Rothman DL, Benveniste H (2012) Metabolomic profiling of children's brains undergoing general anesthesia with sevoflurane and propofol. *Anesthesiology* 117:1062–1071
  15. Zhang J, Zhou W, Qiao H (2011) Bioenergetic homeostasis decides neuroprotection or neurotoxicity induced by volatile anesthetics: a uniform mechanism of dual effects. *Med Hypotheses* 77:223–229
  16. Kodama M, Satoh Y, Otsubo Y, Araki Y, Yonamine R, Masui K, Kazama T (2011) Neonatal desflurane exposure induces more robust neuroapoptosis than do isoflurane and sevoflurane and impairs working memory. *Anesthesiology* 115:979–991
  17. Chan EC, Koh PK, Mal M, Cheah PY, Eu KW, Backshall A, Cavill R, Nicholson JK, Keun HC (2009) Metabolic profiling of human colorectal cancer using high-resolution magic angle spinning nuclear magnetic resonance (HR-MAS NMR) spectroscopy and gas chromatography mass spectrometry (GC/MS). *J Proteome Res* 8:352–361
  18. Kind T, Wohlgenuth G, Lee DY, Lu Y, Palazoglu M, Shahbaz S, Fiehn O (2009) FiehnLib—mass spectral and retention index libraries for metabolomics based on quadrupole and time-of-flight gas chromatography/mass spectrometry. *Anal Chem* 81:10038–10048
  19. Eruslanov E, Kusmartsev S (2010) Identification of ROS using oxidized DCFDA and flow-cytometry. *Methods Mol Biol* 594:57–72
  20. Petit JM, Maftah A, Ratinaud MH, Julien R (1992) 10N-nonyl acridine orange interacts with cardiolipin and allows the quantification of this phospholipid in isolated mitochondria. *Eur J Biochem* 209:267–273
  21. Gown AM, Willingham MC (2002) Improved detection of apoptotic cells in archival paraffin sections: immunohistochemistry using antibodies to cleaved caspase 3. *J Histochem Cytochem* 50:449–454
  22. Paradies G, Petrosillo G, Paradies V, Ruggiero FM (2009) Role of cardiolipin peroxidation and  $Ca^{2+}$  in mitochondrial dysfunction and disease. *Cell Calcium* 45:643–650
  23. Smith EE, Jonides J (1999) Storage and executive processes in the frontal lobes. *Science* 283:1657–1661
  24. Yildiz-Yesiloglu A, Ankerst DP (2006) Neurochemical alterations of the brain in bipolar disorder and their implications for pathophysiology: a systematic review of the in vivo proton magnetic resonance spectroscopy findings. *Prog Neuropsychopharmacol Biol Psychiatry* 30:969–995
  25. Caldeira JC, Wu Y, Mameli M, Purdy RH, Li PK, Akwa Y, Savage DD, Engen JR, Valenzuela CF (2004) Fetal alcohol exposure alters neurosteroid levels in the developing rat brain. *J Neurochem* 90:1530–1539
  26. Kahle KT, Simard JM, Staley KJ, Nahed BV, Jones PS, Sun D (2009) Molecular mechanisms of ischemic cerebral edema: role of electroneutral ion transport. *Physiology (Bethesda)* 24:257–265
  27. MacGregor DG, Avshalumov MV, Rice ME (2003) Brain edema induced by in vitro ischemia: causal factors and neuroprotection. *J Neurochem* 85:1402–1411
  28. Zoratti M, Szabò I (1995) The mitochondrial permeability transition. *Biochim Biophys Acta* 1241:139–176
  29. Gunter TE, Pfeiffer DR (1990) Mechanisms by which mitochondria transport calcium. *Am J Physiol* 258:C755–C786
  30. Zamzami N, Hirsch T, Dallaporta B, Petit PX, Kroemer G (1997) Mitochondrial implication in accidental and programmed cell death: apoptosis and necrosis. *J Bioenerg Biomembr* 29:185–193
  31. Serkova N, Christians U, Fogel U, Pfeuffer J, Leibfritz D (1997) Assessment of the mechanism of astrocyte swelling induced by the macrolide immunosuppressant sirolimus using multinuclear nuclear magnetic resonance spectroscopy. *Chem Res Toxicol* 10:1359–1363
  32. Law RO (1998) The role of taurine in the regulation of brain cell volume in chronically hyponatraemic rats. *Neurochem Int* 33:467–472
  33. Zhang Y, Dong Y, Wu X, Lu Y, Xu Z, Knapp A, Yue Y, Xu T, Xie Z (2010) The mitochondrial pathway of anesthetic isoflurane-induced apoptosis. *J Biol Chem* 285:4025–4037
  34. Zhang J, Dong Y, Xu Z, Zhang Y, Pan C, McAuliffe S, Ichinose F, Yue Y, Liang W, Xie Z (2011) 2-Deoxy-D-glucose attenuates isoflurane-induced cytotoxicity in an in vitro cell culture model of H4 human neuroglioma cells. *Anesth Analg* 113:1468–1475
  35. Chicco AJ, Sparagna GC (2007) Role of cardiolipin alterations in mitochondrial dysfunction and disease. *Am J Physiol Cell Physiol* 292:C33–C44
  36. Halliwell B (2001) Role of free radicals in neurodegenerative diseases: therapeutic implications for antioxidant treatment. *Drugs Aging* 18:685–716
  37. Butterfield DA (2002) Amyloid beta-peptide (1-42)-induced oxidative stress and neurotoxicity: implications for neurodegeneration in Alzheimer's disease brain: a review. *Free Radic Res* 36:1307–1313
  38. Yon JH, Carter LB, Reiter RJ, Jevtovic-Todorovic V (2006) Melatonin reduces the severity of anesthesia-induced apoptotic neurodegeneration in the developing rat brain. *Neurobiol Dis* 21:522–530
  39. Boscolo A, Starr JA, Sanchez V, Lunardi N, DiGruccio MR, Ori C, Erisir A, Trimmer P, Bennett J, Jevtovic-Todorovic V (2012) The abolishment of anesthesia-induced cognitive impairment by timely protection of mitochondria in the developing rat brain: the importance of free oxygen radicals and mitochondrial integrity. *Neurobiol Dis* 45:1031–1041
  40. Zhao X, Yang Z, Liang G, Wu Z, Peng Y, Joseph DJ, Inan S, Wei H (2013) Dual effects of isoflurane on proliferation, differentiation, and survival in human neuroprogenitor cells. *Anesthesiology* 118:537–549
  41. Raichle ME, Gusnard DA (2002) Appraising the brain's energy budget. *Proc Natl Acad Sci USA* 99:10237–10239
  42. Tsuji M, Allred E, Jensen F, Holtzman D (1995) Phosphocreatine and ATP regulation in the hypoxic developing rat brain. *Dev Brain Res* 85:192–200
  43. Clark JB (1998) N-Acetyl aspartate: a marker for neuronal loss or mitochondrial dysfunction. *Dev Neurosci* 20:271–276
  44. Bates TE, Strangward M, Keelan J, Davey GP, Munro PM, Clark JB (1996) Inhibition of N-acetylaspartate production: implications for 1H MRS studies in vivo. *NeuroReport* 7:1397–1400
  45. Yon JH, Daniel-Johnson J, Carter LB, Jevtovic-Todorovic V (2005) Anesthesia induces neuronal cell death in the developing rat brain via the intrinsic and extrinsic apoptotic pathways. *Neuroscience* 135:815–827
  46. Klawitter Jelena, Gottschalk Sven, Hainz Carsten et al (2010) Immunosuppressant neurotoxicity in rat brain models: oxidative stress and cellular metabolism. *Chem Res Toxicol* 23:608–619
  47. Ottersen OP, Zhang N, Walberg F (1992) Metabolic compartmentation of glutamate and glutamine: morphological evidence obtained by quantitative immunocytochemistry in rat cerebellum. *Neuroscience* 46:519–534
  48. Manahan-Vaughan D, Wildförster V, Thomsen C (2008) Rescue of hippocampal LTP and learning deficits in a rat model of psychosis by inhibition of glycine transporter-1 (GlyT1). *Eur J Neurosci* 28:1342–1350
  49. Stratmann G, May LDV, Sall JW, Alvi RS, Bell JS et al (2009) Effect of hypercarbia and isoflurane on brain cell death and neurocognitive dysfunction in 7-day-old rats. *Anesthesiology* 110:849–861
  50. Deng M, Hofacer RD, Jiang C, Joseph B, Hughes EA, Jia B, Danzer SC, Loepke AW (2014) Brain regional vulnerability to anaesthesia-induced neuroapoptosis shifts with age at exposure and extends into adulthood for some regions. *Br J Anaesth* 113:443–451